nanomaterials

MDPI

Article

Effect of Atmospheric Temperature on Epoxy Coating Reinforced with Carbon Nanotubes for De-Icing on Road Systems

Seung-Jun Lee [1], Yu-Jin Jung [2], Chunhee Cho [3,*] and Sung-Hwan Jang [2,4,*]

[1] Department of Civil and Environmental Engineering, Hanyang University, Seoul 04763, Republic of Korea; sj5523@hanyang.ac.kr
[2] Department of Smart City Engineering, Hanyang University ERICA, Ansan 15588, Republic of Korea; yujin0421@hanyang.ac.kr
[3] Department of Civil and Environmental Engineering, University of Hawaii at Manoa, Honolulu, HI 98622, USA
[4] Department of Civil and Environmental Engineering, Hanyang University ERICA, Ansan 15588, Republic of Korea
* Correspondence: chunhee@hawaii.edu (C.C.); sj2527@hanyang.ac.kr (S.-H.J.)

Abstract: Traffic accidents caused by road icing are a serious global problem, and conventional de-icing methods like spraying chemicals have several limitations, including excessive manpower management, road damage, and environmental pollution. In this study, the carbon nanotubes reinforced de-icing coating for the road system with a self-heating function was developed as part of the development of a new system to prevent accidents caused by road icing. The electrical characteristics of the fabricated coating were analyzed, and the carbon nanotube coating heating performance experiment was conducted to measure the temperature increments by applying a voltage to the coating at a sub-zero temperature using an environmental chamber. In addition, the coating was installed on the road pavement and the applicability was investigated through a heating test in winter. As a result of the experiment, the coating made with the higher carbon nanotube concentration presented higher heating owing to its higher electrical conductivity. In addition, the coating showed sufficient heating performance, although the maximum temperature by Joule heating decreased for the entire coating at sub-zero temperatures. Finally, field tests demonstrated the potential of electrically conductive coatings for de-icing applications.

Keywords: carbon nanotube; CNT/EP coating; de-icing; Joule heating

check for updates

Citation: Lee, S.-J.; Jung, Y.-J.; Cho, C.; Jang, S.-H. Effect of Atmospheric Temperature on Epoxy Coating Reinforced with Carbon Nanotubes for De-Icing on Road Systems. *Nanomaterials* **2023**, *13*, 2248. https://doi.org/10.3390/nano13152248

Academic Editor: Muralidharan Paramsothy

Received: 10 July 2023
Revised: 31 July 2023
Accepted: 31 July 2023
Published: 3 August 2023

Copyright: © 2023 by the authors. Licensee MDPI, Basel, Switzerland. This article is an open access article distributed under the terms and conditions of the Creative Commons Attribution (CC BY) license (https://creativecommons.org/licenses/by/4.0/).

1. Introduction

Road systems face their greatest challenges during the winter season in many countries because snowfalls and icing create serious problems in the field of road systems. These challenges involve the mobility of vehicles and the assurance of driver safety. In addition, many road departments are not prepared to immediately remove snow and ice. As a result, snow and ice accumulation on road systems lead to significant financial setbacks. For example, persistent snowfall in northwestern Germany resulted in more than 2000 traffic accidents and a direct economic loss of 100 million Euros in November 2005, and traffic in the northeastern United States was paralyzed by a snowstorm for four days, with a direct economic loss of US $10 billion in January 1996 [1,2]. Considering the financial consequences and threats to public safety, extensive global research has been conducted on various snow and ice removal methods, including their practical implementations. Typical approaches for eliminating snow and ice involve combining the use of deicing chemicals with mechanical extraction techniques. However, these techniques come with drawbacks such as storage and acquisition expenses, extensive labor requirements, environmental harm, and potential damage to the road infrastructure [3–6]. For example, the salty runoff

from road surface deicing operations is responsible for soil and water contamination and adverse health effects for human, plant, and aquatic life [7–12]. In addition, deicing substances account for the largest portion of greenhouse gas emissions related to traditional deicing techniques [13,14]. Globally, the consumption of deicing materials has continuously increased over the past few years which creates serious environmental problems [15].

To address these issues, many research efforts have been devoted to finding cleaner techniques for safely deicing road systems during winter. Some of the emerging techniques involve the application of embedding electrically heated sheet/grille elements inside the road [16] and the application of heated road systems [17–22]. In recent years, conductive composite materials based on carbon nanotubes has attracted attention to improve road systems during winter [23,24]. Dispersing these types of nanoparticles into polymeric structures can enhance thermal stability, resistance to photooxidation, and mechanical attributes, whilst also equipping the resulting nanocomposites with the capacity to exhibit functional properties [25–27]. In recent years, carbon nanotubes (CNTs) have been used in various fields as fillers and CNT-reinforced composites have been confirmed as an alternative de-icing approach. Joule-heating effects occurs when electrical current is passed through conductive composites. CNTs demonstrate a significant self-heating effect when an electric current is applied [28–30]. Joule-heating capabilities have been reported for over a decade. Jang and Park [31] suggested the use of composite materials reinforced with carbon nanotubes, designed for dual purposes like temperature detection and ice removal. Their study showed the feasibility of CNT-reinforced polymer composites for coating systems capable of detecting freezing temperature and self-heating. Yum et al. [32] proposed multi-functional road coating material substances composed of carbon nanotubes (CNTs) and a polyurethane (PU) matrix, commonly used materials in road marking. Prolongo et al. [33] and Redondo et al. [34] proposed the doping of epoxy resins with graphene nanoplatelets as coatings (GNP, 8–10 wt.%) or CNTs (0.1–0.5 wt.%) for the heating of epoxy resin by the Joule effect. In their study, CNTs exhibited greater efficiency in deicing and anti-icing applications owing to their superior electrical conductivity, achieving higher temperatures at reduced electrical voltages. Meanwhile, GNPs generated lower yet more evenly distributed heat. However, studies on carbon nanotube-based heating composites are mainly conducted at room temperature and since they are laboratory-scale studies, it is necessary to study the effect of the atmospheric environment on heating performance and consider large-scale applications.

In our research, we developed a novel coating comprising carbon nanotubes and an epoxy matrix capable of replacing conventional methods of de-icing road systems. We investigated the heating performance of the coating according to atmospheric temperature and its potential applicability through field experiments. We began by examining the electrical properties of the CNT/EP coatings in relation to varying CNT concentrations. Following that, we assessed the heating efficiency of the CNT/EP coating at room temperature, utilizing the Joule effect. To explore the impact of atmospheric temperatures, we measured the heating temperature of the CNT/EP coating under below-freezing conditions. Furthermore, we evaluated the coating's applicability by observing its performance during winter.

2. Experimental

2.1. Materials

In this study, multi-walled carbon nanotubes were adopted from Nanolab, Inc. (Waltham, MA, USA). The CNTs have a purity of higher than 85 wt.% (industrial grade), a diameter of 15 nm, and a length of 5–20 μm. Epoxy was sourced from Easy Composites Ltd. (EpoxAcast 690, Staffordshire, UK), exhibiting a density ranging between 1.12–1.18 g/cm^3 and a viscosity of 200–450 mPa·s. The dispersant used acetone with a purity of 99.7% from Samchun Pure Chemical Co., Ltd. (Pyeongtaek-si, Gyeonggi-do, Republic of Korea).

2.2. Fabrication Procedure

The CNT/EP coating was fabricated following the procedure shown in Figure 1 [35]. A mixture was created by adding 50 g of acetone and 20 g of epoxy resin to a 200 mL beaker, then manually stirring with a stick. Then, varying concentrations of CNTs (0–5 wt.%) were introduced into the beaker and mixed in the same manner (i). An ultrasonicator (Q700CA, Qsonica LLC, Newtown, CT, USA) was then employed to effectively distribute the CNTs within the solution. For this experiment, the ultrasonicator was operated in pulse mode at 90% amplitude for a duration of 30 min (ii). To prevent the acetone from evaporating because of heat, the beaker was surrounded by ice. After dispersion, the sample was placed on a hot plate (60 °C) for 24 h to completely evaporate acetone (iii). Then, 6 g of curing agent was added to the sample and mixed evenly in a 3–roll mill (TR 50M, Trilos, San Ramon, CA, USA) (iv). Following the molding process (v), the sample was positioned within a vacuum chamber for 30 min to eliminate any air bubbles present within the sample (vi).

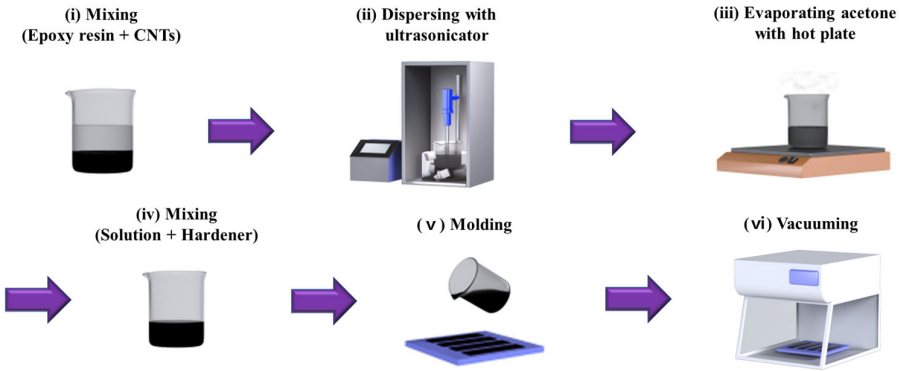

Figure 1. Fabrication procedure for CNT/EP coating.

2.3. Characterization

The heating performance due to the Joule effect is based on the electrical conductivity and the applied voltage of the application. Therefore, in our study, we have set the concentration of CNTs and the applied voltage as the main parameters. The resistance of CNT/EP coatings was gauged using a Keithley 2700 (Tektronix, Beaverton, OR, USA) for standard resistance, and a Keithley 2450 (Tektronix, Beaverton, OR, USA) for high resistance levels exceeding 10^9 Ω. Electrical resistance was assessed based on the current–voltage curves acquired by applying voltages ranging from −10 V to +10 V. The test coating samples were prepared in various CNT concentrations (0.63–5.00 wt.%) with dimensions of 50 mm × 30 mm × 2 mm. High-purity silver paint was applied to both ends of the coating samples to reduce the contact resistance between the coating and the probe point. The electrical conductivity (σ) of the specimens was calculated by $\sigma = L/RA$, where L is the length of the coating (m), R is the resistance of the coating (Ω), and A is the area of the coating (m^2) [36,37]. The microstructure of the CNT/EP coatings was examined by observing the cross-section of the sample under a scanning electron microscope (MIRA3 FE-SEMs from TESCAN, based in Brno, Czech) operating at 15 kV. The cross-section of the coating was coated with platinum using sputter coating (QUORUMQ150T S, Laughton, UK) for 10 min in preparation for a measurement with a magnification of greater than 10,000 times.

As shown in Figure 2a, a voltage-adjustable DC power supply (2260B–800–1, Tektronix, Beaverton, OR, USA) provides electrical energy which is then transformed into thermal energy via the CNT/EP coating. On both ends of the CNT/EP coatings (4–row parallel type: 100 mm × 20 mm × 5 mm), two pieces of copper tape were affixed, intended to function as electrodes, and the input voltage (5–30 V) was applied to the composite to induce heat, creating uniform heat distribution.

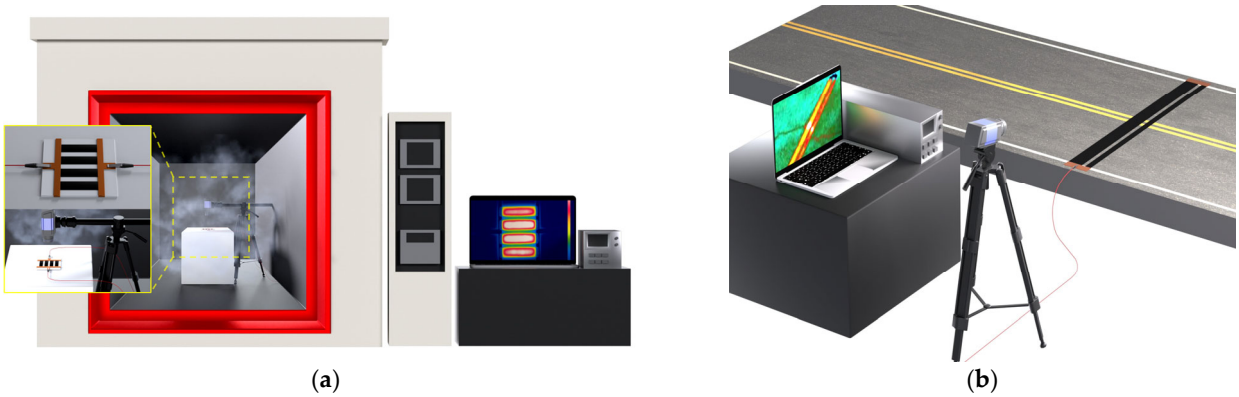

(**a**) (**b**)

Figure 2. Equipment and details of the heating test; (**a**) effect of atmospheric temperature test; (**b**) application test on the road in winter.

A thermal infrared camera (FLIR A655sc, Wilsonville, OR, USA) was used to record the heat distribution across the samples during Joule heating, resulting in thermal images. To investigate the effect of atmospheric temperature on the heating performance, the infrared thermal imaging camera and CNT/EP coating were set in the environmental chamber, and the temperature increments of the CNT/EP coating by applied voltage was measured with respect to the environmental temperature (−20 °C to +20 °C) as shown in Figure 2a. For the field test, CNT/EP coating (5.0 wt.%) was printed on the road. The sizes of the coating were 80 mm × 3000 mm × 5 mm or 40 mm × 3000 mm × 5 mm depending on the actual road width. To examine the heating efficiency of the coating under below-freezing conditions, a study was conducted to observe the relationship between the coating's temperature rise and the voltage applied. This experiment took place during winter with an ambient temperature of approximately −8 °C. Figure 2b presented the experimental setup for the heating performance of the CNT/EP coating application in the field test.

3. Results and Discussion

3.1. Electrical Characteristics of CNT/EP Coating

The addition of CNT in the epoxy metrics can significantly improve the electrical conductivity of the coating because of the superior electrical conductivity and high aspect ratio of the CNT [38]. The electrical conductivity of the CNT/EP coatings was measured for various CNT concentrations as shown in Figure 3a. In general, materials with electrical conductivities below about 10^{-8} S/m are insulator, and those with electrical conductivities above 10^{-8} S/m are conductive. At low concentration, lower than 0.25 wt.% of CNTs, the coatings showed non-conductivity. The electrical conductivity of the coating rapidly increased when the CNT concentration rose to between 0.25 to 1.0 wt.% based on increases in the CNT networks. This sharp increase in the electrical conductivity of CNT/EP coating is because of the formation of a percolation threshold [39–42]. In this study, the percolation threshold, which is the minimum CNT concentration in the matrix after which there is no significant change in electrical conductivity, occurred at approximately 0.63 wt.% CNTs. The effectiveness of electron transfer between CNTs is highly dependent on the CNTs spacing distance. After 1.0 wt.%, the electrical conductivity increased only gradually, showing saturation. Figure 3b shows the microstructure of the 5 wt.% coating. These distributions of the CNTs within the epoxy matrix contribute high and stable electrical conductivity of the CNT/EP coatings.

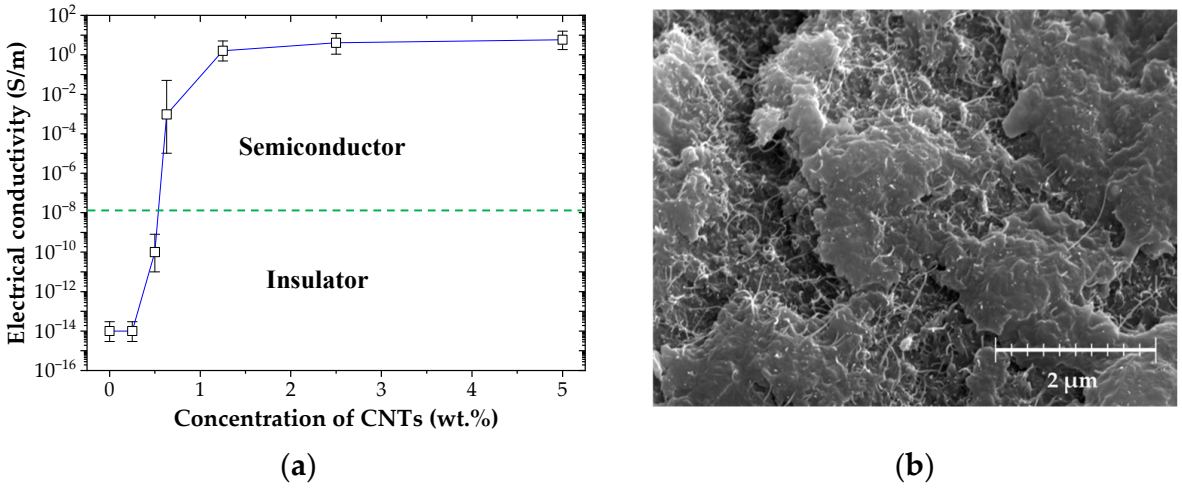

Figure 3. Electrical characteristics of CNT/EP coating; (**a**) electrical conductivity; (**b**) SEM image.

3.2. Heating Characteristics of CNT/EP Coating at Room Temperature

According to Joule's law, the CNT/EP coating converts electric energy into thermal energy after loading voltage, which mainly shows rapidly increasing temperature stage of the coating [43,44]. Figure 4a–d shows the time–temperature curve of the CNT/EP coating at room temperature (20 °C). As observed, a fast temperature increase of the coatings is seen in the first five minutes. Following this, the temperature gradient in time is reduced, indicating stability of the heat transfer process. Furthermore, the higher the CNT concentration, the higher the temperature response. The results show that the coatings showed high heating performance as the CNT concentration and voltage increased. In particular, increasing the CNT concentration to 5.00 wt.% CNT/EP coating results in a heating temperature range of 20.1–184.4 °C under 5–30 V. Figure 4e showed the temperature increment and distribution with CNT concentrations at room temperature. This figure depicts all CNT concentration heating tests in which a fixed voltage of 30 V was applied. It shows an even temperature distribution of the coatings according to the applied voltage. These results suggest that CNTs are well-dispersed in the epoxy matrix [45]. Figure 4g shows the maximum temperature of the CNT/EP coating at room temperature as a function of applied voltage. The maximum temperature of the coating increases nonlinearly as the voltage and the CNT concentration increase. These results are supported by the Joule effect ($Q = I^2Rt = V^2t/R$, where Q is Joule heat, I is current, R is resistance, V is applied voltage and t is operating time). Another important aspect of the Joule heating system is the heating ratio [45,46]. Figure 4f shows the heating ratio of the coating during the first 30 s. The heating ratio increases rapidly with the increase of CNT concentration and the applied voltage. For example, the heating ratio is 0.17, 0.51, and 1.61 °C/s for coatings with 1.25, 2.50, and 5.00 wt.% coatings when applied 30 V, respectively. This high initial heating ratio of the CNT/EP coating is suitable for rapid de-icing.

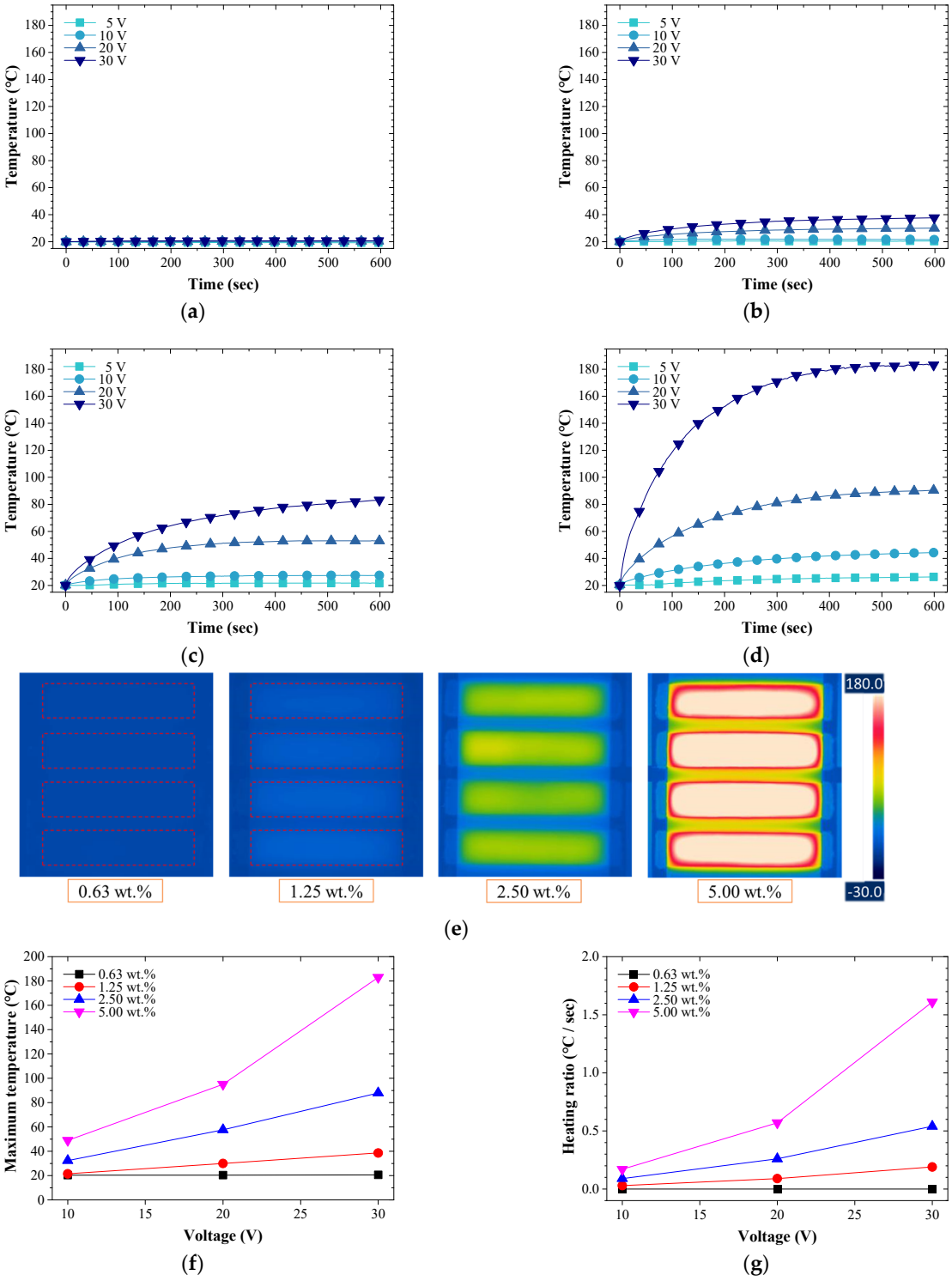

Figure 4. Heating characteristics of the CNT/EP coating at room temperature; (**a**) 0.63 wt.%; (**b**) 1.25 wt.%; (**c**) 2.50 wt.%; (**d**) 5.00 wt.%; (**e**) heating distribution; (**f**) maximum temperature; (**g**) heating ratio during the first 30 s.

To evaluate the applicability of CNT/EP coatings based on Joule heating, a deeper exploration of thermal efficiency is required, as it signifies the de-icing capability in relation to the energy consumed. Figure 5 shows the energy characteristics of CNT/EP coating according to the applied voltage and CNT concentration. The electric power is calculated by $P = V^2/R$. The relationship between the applied voltage and the power is comparable to

that between the maximum temperature of the coating and the voltages shown in Figure 4f. This indicates that most of the electric power applied to the coatings was transformed into heat during the electric heating experiments [34,47]. To evaluate the energy efficiency, the power density (W·cm^{-3}) can be calculated as electric power per unit volumetric [48,49]. Figure 5a shows the temperature increments of CNT/EP coating by applied voltages as a function of power density. The temperature increase produced by the CNT/EP coating is linearly related to the power density, indicating high compliance with Joule law [50]. The slope of achieved temperature versus power density provides thermal efficiency, an important factor to evaluate the heating performance of a heater [51–53]. A larger slope value indicates that less energy is required to increase the temperature, thereby being indicative of higher thermal efficiency. Figure 5b shows the results of the thermal efficiency of the CNT/EP coating. The 1.25 wt.% coating had the highest thermal efficiency, and the thermal efficiency gradually decreased with CNT concentration. This result can be explained by the higher maximum temperature intensifying the heat exchange with the coating and its surroundings. Importantly, the thermal efficiency of the coating is quite high compared with similar systems reported in other literature [54,55]. This result shows that the CNT/EP coating has high thermal efficiency by attaining maximum temperatures with relatively low electric power.

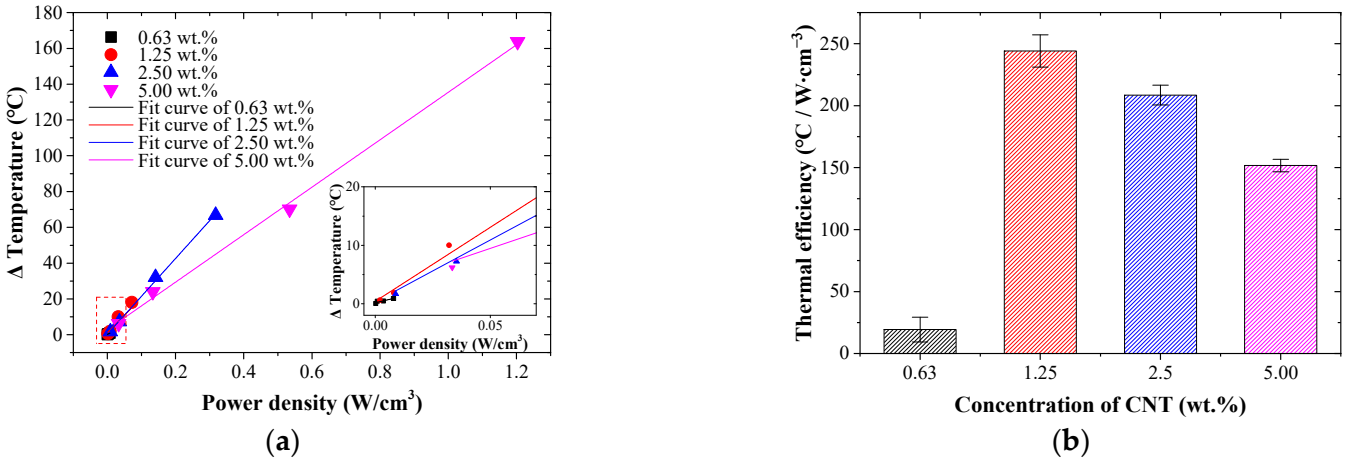

Figure 5. Energy characteristics for heating of CNT/EP coating; (**a**) temperature increase by power density; (**b**) thermal efficiency.

3.3. Effect of Atmospheric Temperatures on Heating Performance of CNT/EP Coating

Many studies related to Joule heating performance of CNT composites have been conducted [56–59]. However, most studies have investigated the heating performance of CNT composites at room temperature or at a fixed temperature level. Only a few studies on the effects of the atmospheric temperature have studied heating performance. In this study, the heating performance of the CNT/EP coatings was investigated at various environmental temperatures to evaluate the effect of atmospheric temperature. Figure 6a shows the temperature change on the coating (1.25–5.00 wt.%) increases with respect to the atmospheric temperature when a voltage of 30 V is applied. On the contrary, the temperature change on the coating decreased significantly as the atmospheric temperature decreased. In the case of 5.00 wt.%, the maximum temperature increment of the coating was reduced by about 29% at −20 °C compared to room temperature (20 °C). Low atmospheric temperature affected not only the maximum heat temperature but also the heating ratio. Figure 6b shows the temperature of the coatings over time when a voltage of 30 V was applied at room temperature and −20 °C. The heating ratio also significantly decreased by 31–43% according to the lower atmospheric temperature compared to the heating ratio at room temperature. Figure 6c shows the heating test results at −20 °C and revealed an even temperature distribution like the room temperature test results, but the overall temperature

increment was reduced. As a result, some results did not reach the zero temperature. For example, the 1.25 wt.% coating had the highest thermal efficiency from previous results but did not reach the temperature required for de-icing of −20 °C. This result indicates coatings too low in concentration are not suitable as CNT/EP coatings in low temperature environments. The decrease in temperature is due to various influences, one of which is the creation of the frost as the atmospheric temperature decreases. When the surface temperature of the coating is below the water freezing temperature, the transferred water vapor may condense and then freeze on the cold surface [60,61]. This frost affects the lowering of Joule heating [62]. Another factor could be the resistance properties of the coating according to temperature. Figure 6d shows the result of coating resistance with decreasing atmospheric temperature. The CNT/EP coating showed a negative temperature coefficient with increasing resistance of all coatings with decreasing environmental temperature [31,63]. This increase in resistance causes a decrease in the electrical power, which can decrease in thermal efficiency. Figure 6e shows the thermal efficiency of the coating according to the atmospheric temperature. As the atmospheric temperature decreased, the thermal efficiency of all coatings decreased from about 30–37%. Although the heating performance deteriorated owing to the environmental temperature, the CNT/EP coating still showed high heating performance. These results mean that the CNT/EP coating can be applied even in extreme environments. Furthermore, to apply de-icing systems using Joule heating as well as the proposed CNT/EP coating, we must investigate the effect of atmospheric temperature on the heating performance.

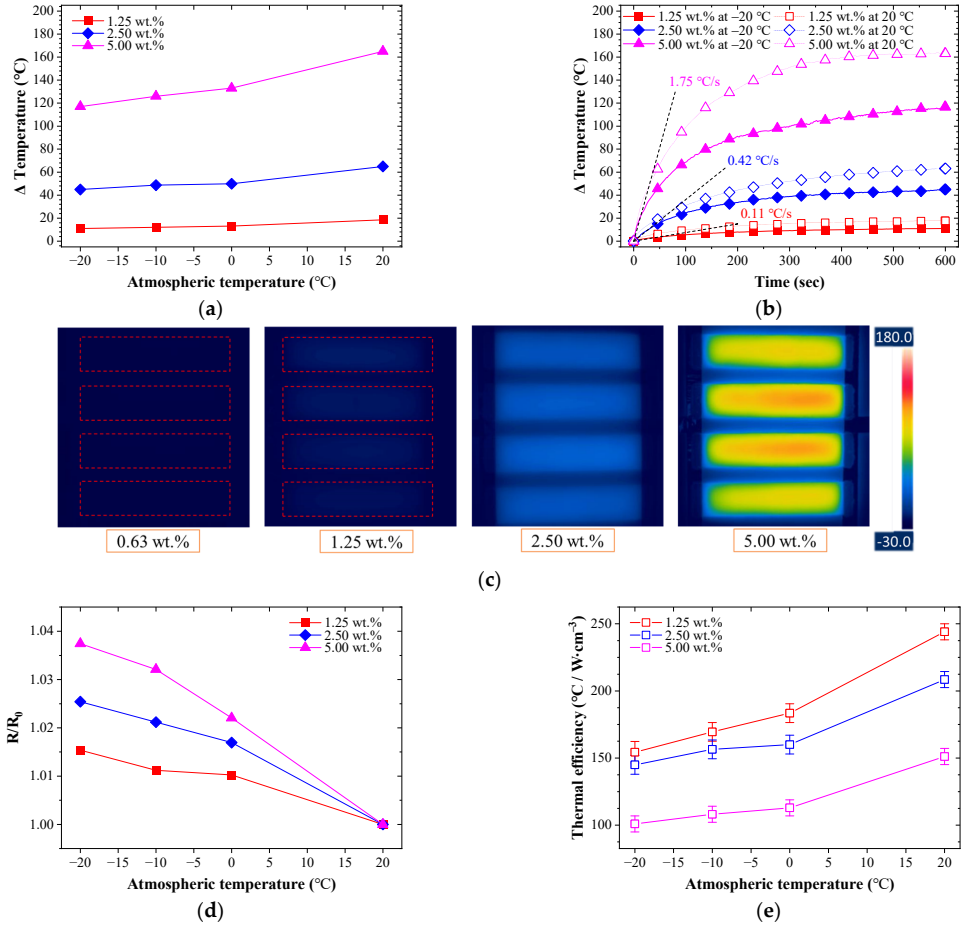

Figure 6. Effect of the atmospheric temperature on CNT/EP coating; (**a**) maximum temperature increments by 30 V; (**b**) comparison of heating performance for −20 °C and room temperature; (**c**) infrared image at −20 °C; (**d**) normalized resistance; (**e**) thermal efficiency.

3.4. Application of Road Heating System

To demonstrate the feasibility of the proposed method, we placed CNT/EP coating on the road pavements as shown in Figure 7a. The 5.00 wt.% coating was used as the highest heating value. After installation, heating performance of CNT/EP coating was measured by 220 V at −8 °C air temperature. This is to compare the heating performance by applying power like the experiment in which 30 V was applied to the 5.0 wt.% concentration of the laboratory-scale sample (about 50 W). Figure 7b showed the temperature increments of CNT/EP coating by applied voltage for 20 min. Figure 7c,d shows the thermal images of the CNT/EP coating at times t_0 and t_1, respectively. The resistance of EC01 and EC02 was 960 Ω and 1960 Ω at 20 °C, respectively. The resistance of EC02 is about twice that of EC01. The experiment was carried out during an evening in winter 2021. As a result of the heating test, the surface temperature of the coating increased above 10 °C from about −5 °C. After the voltage was applied, it heated up rapidly for 200 s, and the EC01 sample showed a higher temperature than EC02. It should show a similar heating pattern for the same applied voltage, but the EC01 sample showed a higher and more even temperature. This is because the dispersion of the CNTs in EC01 sample was more evenly distributed than that of the EC02 sample which can be confirmed by comparing the heating distribution of the coating as shown in Figure 7d. As the coating size increases, the thermal efficiency is lower than that of laboratory-scale samples, but it is possible to heat above zero depending on the applied voltage from sub-zero temperature. In addition, it is possible to increase power efficiency by optimizing the coating standard, and, evidenced through these studies, can be used as a road heating coating. Figure 8 shows a concept of the CNT/EP coating system for road de-icing. It comprises a heating coating that removes icing and a control system that applies voltage when icing occurs. Through this system, it is possible to achieve active, efficient, and eco-friendly ice removal unlike conventional methods such as spraying chemicals.

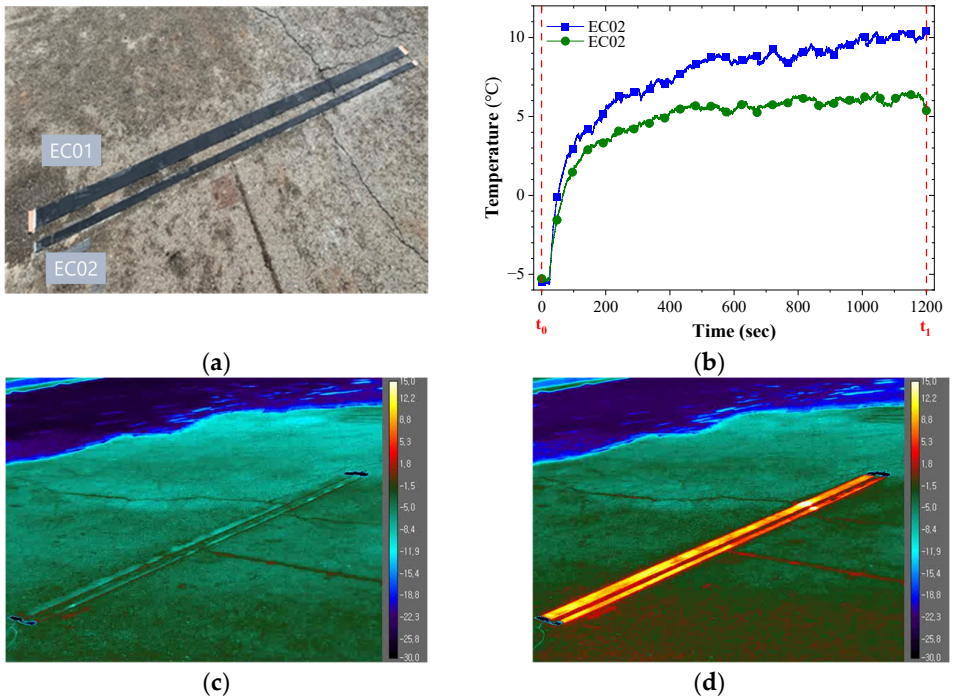

Figure 7. Application for CNT/EP coating on the road; (**a**) painting the coating on the road; (**b**) temperature increments; (**c**) surface temperature at t_0; (**d**) surface temperature at t_1.

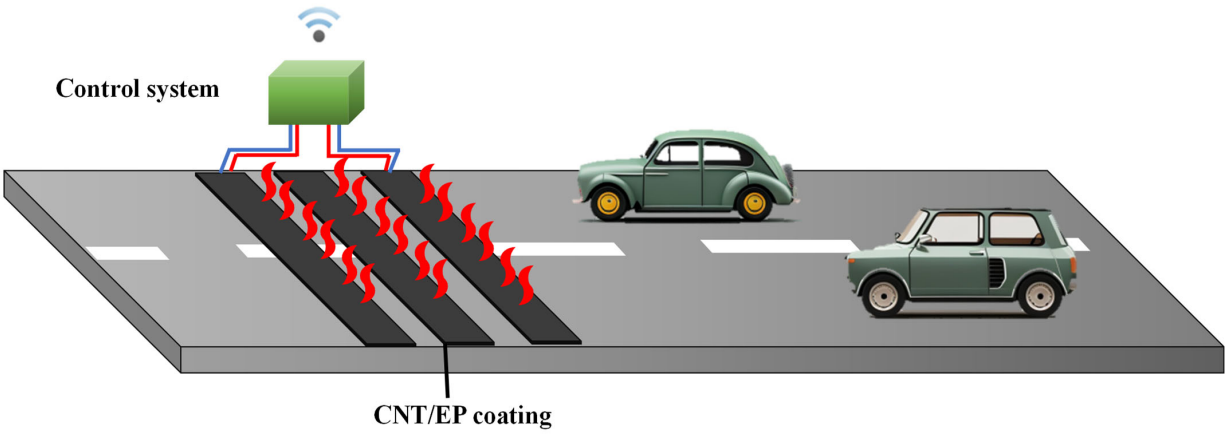

Figure 8. A concept of the CNT/EP coating system for road de-icing.

4. Conclusions

The aim of this study was to examine the relationship between the concentration of CNTs and supply voltage with respect to the heating and electrical performance of CNT/EP coating, and to assess the impact of atmospheric temperature on this relationship. The goal was to provide an alternative solution to the issues caused by chemical de-icing agents in road systems. By dispersing CNTs in an epoxy matrix, we have successfully fabricated highly electrically conductive coatings. Measurement of the variation of electrical conductivity with CNT concentration showed that the percolation threshold occurred when CNT concentration was between 0.5 wt.% and 1.0 wt.%. To evaluate the applicability of CNT/EP coatings based on Joule heating, thermal efficiency was investigated at room temperature, as it signifies the de-icing capability in relation to the energy consumed. Results show that the CNT/EP coating has high thermal efficiency by attaining maximum temperatures with relatively low electric power. As a result of the heating test of the CNT/EP coating according to atmospheric temperature, it was found that a decrease in atmospheric temperature reduced the heating performance of the coating. Nevertheless, it was confirmed that the heating performance of the coating remained above freezing even under sub-zero temperatures. Finally, application tests confirmed that the de-icing coating developed and verified in this study present good heating performance and applicability. As a result of the application test at sub-zero temperature, it was proved that the coating can reach the de-icing temperature and it is possible to respond according to the installation environment. Through these results, it was confirmed that the developed coating could be used not only to prevent ice on the road system as an eco-friendly coating but also may be applied to structures in various fields.

Author Contributions: Conceptualization, S.-H.J.; methodology, S.-H.J.; formal analysis, S.-H.J.; investigation, S.-J.L. and S.-H.J.; writing—original draft preparation, S.-J.L.; writing—review and editing, C.C. and S.-H.J.; visualization, S.-J.L. and Y.-J.J.; supervision, C.C. and S.-H.J.; project administration, S.-H.J.; funding acquisition, S.-H.J. All authors have read and agreed to the published version of the manuscript.

Funding: This work was supported by the research fund of Hanyang University (HY–202200000002564) and the National Research Foundation of Korea (NRF) grant funded by the Korea government (MSIT) (NRF–2020R1C1C1005273).

Institutional Review Board Statement: Not applicable.

Informed Consent Statement: Not applicable.

Data Availability Statement: Not applicable.

Conflicts of Interest: The authors declare no conflict of interest.

References

1. Vitaliano, D.F. An economic assessment of the social costs of highway salting and the efficiency of substituting a new deicing material. *J. Policy Anal. Manag.* **1992**, *11*, 397–418. [CrossRef]
2. Yu, W.; Yi, X.; Guo, M.; Chen, L. State of the art and practice of pavement anti-icing and de-icing techniques. *Sci. Cold Arid Reg.* **2014**, *6*, 14–21.
3. Arabzadeh, A.; Ceylan, H.; Kim, S.; Gopalakrishnan, K.; Sassani, A. Super-hydrophobic coatings on asphalt concrete surfaces. *Transport. Res. Rec. J. Transport. Res. Board.* **2016**, *2551*, 10–17. [CrossRef]
4. Arabzadeh, A.; Ceylan, H.; Kim, S.; Gopalakrishnan, K.; Sassani, A. Fabrication of polytetrafluoroethylene-coated asphalt concrete biomimetic surfaces: A nanomaterials based pavement winter maintenance approach. In Proceedings of the 2016 International Conference on Transportation and Development, Houston, TX, USA, 26–29 June 2016; pp. 54–64.
5. Lai, Y.; Liu, Y.; Ma, D. Automatically melting snow on airport cement concrete pavement with carbon fiber grille. *Cold Reg. Sci. Technol.* **2014**, *103*, 57–62. [CrossRef]
6. Ramakrishna, D.M.; Viraraghavan, T. Environmental impact of chemical deicers—A review. *Water Air Soil Pollut.* **2005**, *166*, 49–63. [CrossRef]
7. Christopher, A.; Strong, J.E.; Mosher, P.A. Effect of deicing salts on metal and organic matter mobilization in roadside soils. *Environ. Sci. Technol.* **1992**, *26*, 703–709.
8. Bäckström, M.; Karlsson, S.; Bäckman, L.; Folkeson, L.; Lind, B. Mobilisation of heavy metals by deicing salts in a roadside environment. *Water Res.* **2004**, *38*, 720–732. [CrossRef]
9. Sanzo, D.; Hecnar, S.J. Effects of road de-icing salt (NaCl) on larval wood frogs (*Rana sylvatica*). *Environ. Pollut.* **2006**, *140*, 247–256. [CrossRef]
10. Czerniawska-Kusza, I.; Kusza, G.; Duzynski, M. Effect of deicing salts on urban soils and health status of roadside trees in the Opole Region. *Environ. Toxicol.* **2004**, *19*, 296–301. [CrossRef]
11. Cunningham, M.A.; Snyder, E.; Yonkin, D.; Ross, M.; Elsen, T. Accumulation of deicing salts in soils in an urban environment. *Urban Ecosyst.* **2008**, *11*, 17–31. [CrossRef]
12. Karraker, N.E.; Gibbs, J.P.; Vonesh, J.R. Impacts of road deicing salt on the demography of vernal pool-breeding Amphibians. *Ecol. Appl.* **2016**, *18*, 724–734. [CrossRef] [PubMed]
13. Shen, W.; Ceylan, H.; Gopalakrishnan, K.; Kim, S.; Taylor, P.C.; Rehmann, C.R. Life cycle assessment of heated apron pavement system operations. *Transport. Res. Road Environ.* **2016**, *48*, 316–331. [CrossRef]
14. Wang, H.; Thakkar, C.; Chen, X.; Murrel, S. Life-cycle assessment of airport pavement design alternatives for energy and environmental impacts. *J. Clean. Prod.* **2016**, *133*, 163–171. [CrossRef]
15. Xu, H.; Tan, Y. Modeling and operation strategy of pavement snow melting systems utilizing low-temperature heating fluids. *Energy* **2015**, *80*, 666–676. [CrossRef]
16. Chang, C.; Ho, M.; Song, G.; Mo, Y.-L.; Li, H. A feasibility study of self-heating concrete utilizing carbon nanofiber heating elements. *Smart Mater. Struct.* **2009**, *18*, 127001. [CrossRef]
17. Farcas, C.; Galao, O.; Navarro, R.; Zornoza, E.; Baeza, F.J.; Del Moral, B.; Pla, R.; Garcés, P. Heating and de-icing function in conductive concrete and cement paste with the hybrid addition of carbon nanotubes and graphite products. *Smart Mater. Struct.* **2021**, *30*, 045010. [CrossRef]
18. Gomis, J.; Galao, O.; Gomis, V.; Zornoza, E.; Garces, P. Self-heating and deicing conductive cement. Experimental study and modeling. *Constr. Build. Mater.* **2015**, *75*, 442–449. [CrossRef]
19. Pan, P.; Wu, S.; Xiao, Y.; Liu, G. A review on hydronic asphalt pavement for energy harvesting and snow melting. *Renew. Sustain. Energy Rev.* **2015**, *48*, 624–634. [CrossRef]
20. Tuan, C.Y. *Implementation of Conductive Concrete for Deicing (Roca Bridge)*; University of Nebraska: Lincoln, NE, USA, 2008.
21. Wang, H.; Liu, L.; Chen, Z. Experimental investigation of hydronic snow melting process on the inclined pavement. *Cold Reg. Sci. Technol.* **2010**, *63*, 44–49. [CrossRef]
22. Xu, H.; Wang, D.; Tan, Y.; Zhou, J.; Oeser, M. Investigation of design alternatives for hydronic snow melting pavement systems in China. *J. Clean. Prod.* **2018**, *170*, 1413–1422. [CrossRef]
23. Han, B.G.; Yu, X.; Kwon, E. A self-sensing carbon nanotube/cement composite for traffic monitoring. *Nanotechnology* **2009**, *20*, 44. [CrossRef] [PubMed]
24. Maurin, L.; Boussoir, J.; Rougeault, S.; Bugaud, M.; Ferdinand, P.; Landrot, A.G.; Grunevald, Y.H.; Chauvin, T. FBG-based smart composite bogies for railway applications. In Proceedings of the 2002 15th Optical Fiber Sensors Conference Technical Digest. OFS 2002 (Cat. No. 02EX533), Portland, OR, USA, 10 May 2002; pp. 91–94.
25. Pujar, N.V.; Nanjundaradhya, N.V.; Sharma, R.S. Effect of graphene oxide nano filler on dynamic behaviour of GFRP composites. In Proceedings of the AIP Conference Proceedings, Lausanne, Switzerland, 19–21 March 2018; Volume 1943.
26. Fouda, H.; Guo, L. The mechanical properties of CF/Epoxy resin composite with adding different types of CNTs. *Int. J. Eng. Res. Technol.* **2017**, *6*, 311–315.
27. Mostovoy, A.; Yakovlev, A.; Tseluikin, V.; Lopukhova, M. Epoxy nanocomposites reinforced with functionalized carbon nanotubes. *Polymers* **2020**, *12*, 1816. [CrossRef] [PubMed]
28. Isaji, S.; Bin, Y.; Matsuo, M. Electrical conductivity and self-temperature-control heating properties of carbon nanotubes filled polyethylene films. *Polymer* **2009**, *50*, 1046–1053. [CrossRef]

29. Kumar, S.; Pimparkar, N.; Murthy, J.Y.; Alam, M.A. Self-consistent electrothermal analysis of nanotube network transistors. *J. Appl. Phys.* **2011**, *109*, 014315. [CrossRef]
30. Chien, A.T.; Cho, S.; Joshi, Y.; Kumar, S. Electrical conductivity and Joule heating of polyacrylonitrile/carbon nanotube composite fibers. *Polymer* **2014**, *55*, 6896–6905. [CrossRef]
31. Jang, S.H.; Park, Y.L. Carbon nanotube-reinforced smart composites for sensing freezing temperature and deicing by CNT/EP. *Nanomater. Nanotechnol.* **2018**, *8*, 1847980418776473. [CrossRef]
32. Yum, S.G.; Yin, H.; Jang, S.H. Toward multi-functional road surface design with the nanocomposite coating of carbon nanotube modified polyurethane: Lab-scale experiments. *Nanomaterials* **2020**, *10*, 1905. [CrossRef]
33. Prolongo, S.G.; Moriche, R.; Del Rosario, G.; Jiménez-Suárez, A.; Prolongo, M.G.; Ureña, A. Joule effect self-heating of epoxy composites reinforced with graphitic nanofillers. *J. Polym. Res.* **2016**, *23*, 189. [CrossRef]
34. Redondo, O.; Prolongo, S.G.; Campo, M.; Sbarufatti, C.; Giglio, M. Anti-icing and de-icing coatings based Joule's heating of graphene nanoplatelets. *Compos. Sci. Technol.* **2018**, *164*, 65–73. [CrossRef]
35. Lee, S.J.; Jung, Y.J.; Park, J.W.; Jang, S.H. Temperature Detectable Surface Coating with Carbon Nanotube/Epoxy Composites. *Nanomaterials* **2022**, *12*, 2369. [CrossRef] [PubMed]
36. Fang, Y.; Li, L.Y.; Jang, S.H. Calculation of electrical conductivity of self-sensing carbon nanotube composites. *Compos. B Eng.* **2020**, *199*, 108314. [CrossRef]
37. Jang, S.H.; Li, L.Y. Self-sensing carbon nanotube composites exposed to glass transition temperature. *Materials* **2020**, *13*, 259. [CrossRef] [PubMed]
38. Jang, S.H.; Kim, D.; Park, Y.L. Accelerated curing and enhanced material properties of conductive polymer nanocomposites by joule heating. *Materials* **2018**, *11*, 1775. [CrossRef]
39. Kim, J.K.; Mai, Y.W. (Eds.) *Engineered Interfaces in Fiber Reinforced Composites*; Elsevier: Amsterdam, The Netherlands, 1998.
40. Vertuccio, L.; Guadagno, L.; Spinelli, G.; Lamberti, P.; Zarrelli, M.; Russo, S.; Iannuzzo, G. Smart coatings of epoxy based CNTs designed to meet practical expectations in aeronautics. *Compos. Part B Eng.* **2018**, *147*, 42–46. [CrossRef]
41. Xin, X.; Liang, M.; Yao, Z.; Su, L.; Zhang, J.; Li, P.; Sun, C.; Jiang, H. Self-sensing behavior and mechanical properties of carbon nanotubes/epoxy resin composite for asphalt pavement strain monitoring. *Constr. Build. Mater.* **2020**, *257*, 119404. [CrossRef]
42. Cataldo, A.; Biagetti, G.; Mencarelli, D.; Micciulla, F.; Crippa, P.; Turchetti, C.; Pierantoni, L.; Bellucci, S. Modeling and electrochemical characterization of electrodes based on epoxy composite with functionalized nanocarbon fillers at high concentration. *Nanomaterials* **2020**, *10*, 850. [CrossRef]
43. Cortés, A.; Romate, X.F.S.; Jiménez-Suárez, A.; Campo, M.; Prolongo, M.G.; Ureña, A.; Prolongo, S.G. 3D printed anti-icing and de-icing system based on CNT/GNP doped epoxy composites with self-curing and structural health monitoring capabilities. *Smart Mater. Struct.* **2020**, *30*, 025016. [CrossRef]
44. Liang, S.; Wang, H.; Tao, X. Multiwalled carbon nanotube/cationic cellulose nanofibril electrothermal films: Mechanical, electrical, electrothermal, and cycling performances. *Wood Sci. Technol.* **2021**, *55*, 1711–1723. [CrossRef]
45. Farcas, C.; Galao, O.; Vertuccio, L.; Guadagno, L.; Romero-Sánchez, M.D.; Rodríguez-Pastor, I.; Garcés, P. Ice-prevention and de-icing capacity of epoxy resin filled with hybrid carbon-nanostructured forms: CNT/EP by Joule effect. *Nanomaterials* **2021**, *11*, 2427. [CrossRef]
46. Lee, T.W.; Jeong, Y.G. Regenerated cellulose/multiwalled carbon nanotube composite films with efficient electric heating performance. *Carbohydr. Polym.* **2015**, *133*, 456–463. [CrossRef]
47. An, J.E.; Jeong, Y.G. Structure and electric heating performance of graphene/epoxy composite films. *Eur. Polym. J.* **2013**, *49*, 1322–1330. [CrossRef]
48. Lee, H.B.; Veerasubramani, G.K.; Lee, K.S.; Lee, H.; Han, T.H. Joule heating-induced faradaic electrode-decorated graphene fibers for flexible fiber-shaped hybrid supercapacitor with high volumetric energy density. *Carbon* **2022**, *198*, 252–263. [CrossRef]
49. Wang, B.; Wang, G.F.; Jiang, S.S.; Zhang, K.F. Effect of pulse current on thermal performance and deep drawing of SiCp/2024Al composite sheet. *Int. J. Adv. Manuf. Technol.* **2013**, *67*, 623–627. [CrossRef]
50. Zhou, B.; Han, X.; Li, L.; Feng, Y.; Fang, T.; Zheng, G.; Wang, B.; Dai, K.; Liu, C.; Shen, C. Ultrathin, flexible transparent Joule heater with fast response time based on single-walled carbon nanotubes/poly(vinyl alcohol) film. *Compos. Sci. Technol.* **2019**, *183*, 107796. [CrossRef]
51. Zhang, X.; Wang, X.; Lei, Z.; Wang, L.; Tian, M.; Zhu, S.; Xiao, H.; Tang, X.; Qu, L. Flexible MXene-decorated fabric with interwoven conductive networks for integrated Joule heating, electromagnetic interference shielding, and strain sensing performances. *ACS Appl. Mater. Interfaces* **2020**, *12*, 14459–14467. [CrossRef]
52. Zhou, B.; Li, Z.; Li, Y.; Liu, X.; Ma, J.; Feng, Y.; Zhang, D.; He, C.; Liu, C.; Shen, C. Flexible hydrophobic 2D Ti3C2Tx-based transparent conductive film with multifunctional self-cleaning, electromagnetic interference shielding and joule heating capacities. *Compos. Sci. Technol.* **2021**, *201*, 108531. [CrossRef]
53. Sun, Y.; Ding, R.; Hong, S.Y.; Lee, J.; Seo, Y.K.; Nam, J.D.; Suhr, J. MXene-xanthan nanocomposite films with layered microstructure for electromagnetic interference shielding and Joule heating. *Chem. Eng. J.* **2021**, *410*, 128348. [CrossRef]
54. Jeong, Y.G.; An, J.E. Effects of mixed carbon filler composition on electric heating behavior of thermally-cured epoxy-based composite films. *Compos. Part A Appl. Sci. Manuf.* **2014**, *56*, 1–7. [CrossRef]

55. Wang, F.X.; Liang, W.Y.; Wang, Z.Q.; Yang, B.; He, L.; Zhang, K. Preparation and property investigation of multi-walled carbon nanotube (MWCNT)/epoxy composite films as high-performance electric heating (resistive heating) element. *Express Polym. Lett.* **2018**, *12*, 285–295. [CrossRef]
56. Tang, P.; Zhang, R.; Shi, R.; Bin, Y. Synergetic effects of carbon nanotubes and carbon fibers on electrical and self-heating properties of high-density polyethylene composites. *J. Mater.* **2015**, *50*, 1565–1574. [CrossRef]
57. Prolongo, S.G.; Moriche, R.; Jiménez-Suárez, A.; Delgado, A.; Ureña, A. Printable self-heating coatings based on the use of carbon nanoreinforcements. *Polym. Compos.* **2020**, *41*, 271–278. [CrossRef]
58. Chu, H.; Zhang, Z.; Liu, Y.; Leng, J. Self-heating fiber reinforced polymer composite using meso/macropore carbon nanotube paper and its application in deicing. *Carbon* **2014**, *66*, 154–163. [CrossRef]
59. Xu, C.; Xu, S.; Eticha, R.D. Experimental investigation of thermal performance for pulsating flow in a microchannel heat sink filled with PCM (paraffin/CNT composite). *Energy Convers. Manag.* **2021**, *236*, 114071. [CrossRef]
60. Brian, P.T.; Reid, R.C.; Shah, Y.T. Frost deposition on cold surfaces. *Ind. Eng. Chem. Fund.* **1970**, *9*, 375–380. [CrossRef]
61. Na, B.; Webb, R.L. A fundamental understanding of factors affecting frost nucleation. *Int. J. Heat Mass Transf.* **2003**, *46*, 3797–3808. [CrossRef]
62. Liebscher, M.; Tzounis, L.; Junger, D.; Dinh, T.T.; Mechtcherine, V. Electrical Joule heating of cementitious nanocomposites filled with multi-walled carbon nanotubes: Role of filler concentration, water content, and cement age. *Smart Mater. Struct.* **2020**, *29*, 125019. [CrossRef]
63. Li, Q.; Xue, Q.Z.; Gao, X.L.; Zheng, Q.B. Temperature dependence of the electrical properties of the carbon nanotube/polymer composites. *Express Polym. Lett.* **2009**, *3*, 769–777. [CrossRef]

Disclaimer/Publisher's Note: The statements, opinions and data contained in all publications are solely those of the individual author(s) and contributor(s) and not of MDPI and/or the editor(s). MDPI and/or the editor(s) disclaim responsibility for any injury to people or property resulting from any ideas, methods, instructions or products referred to in the content.